Hyperspectral Atmospheric Correction Over Land

Bo-Cai Gao

June 2014

Remote Sensing Division,
Naval Research Laboratory, Washington, DC USA

Brief History on ATREM Algorithm Development

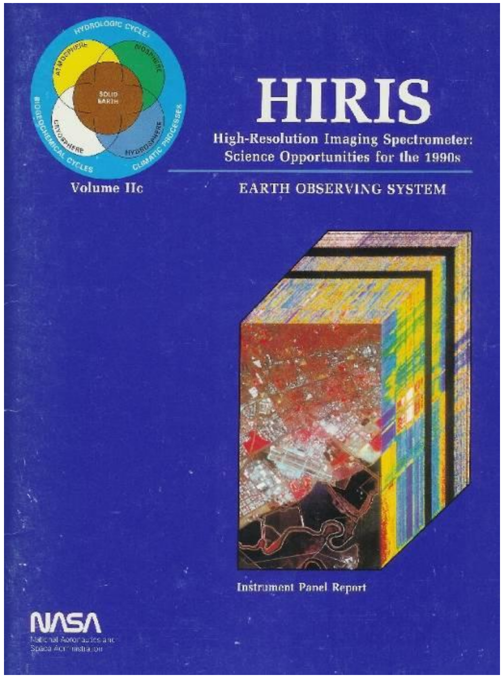

In the late 1980s, MODIS & HIRIS were envisioned to be parts of the massive NASA EOS Program. Professor Alex. Geotz at University of Colorado in Boulder, Colorado was the NASA-selected HIRIS Team leader. He envisioned the need of a model-based atmospheric correction algorithm around 1987.

I worked with Dr. Goetz at U. of Colorado from 1988 to 1992 for the HIRIS Project to develop the 1st band-model-based hyperspectral atmospheric correction algorithm - ATREM. The ATREM source code was publicly released through U. of Colorado to more than 300 researchers worldwide in mid-1990s.

- Timeline of algorithm development:
- ATREM – 1st land version (~1991, band model) to support the AVIRIS/HIRIS Project. A Paper was published in 1993 on RSE.
- ATREM – upgraded land version (~1997, line-by-line model) to support the Navy COIS/NEMO Project. Reported in a 1997 SPIE extended abstract.
- ATREM – 1st ocean version (~1999, line-by-line, spectrum matching using ***channels above 0.86 μm for Case 2 waters***, based on R. Fraser's formulation and multi-layer atmospheric model). A paper was published in 2000 on Applied Optics.

Atmospheric Correction Over Land

An AVIRIS Spectrum

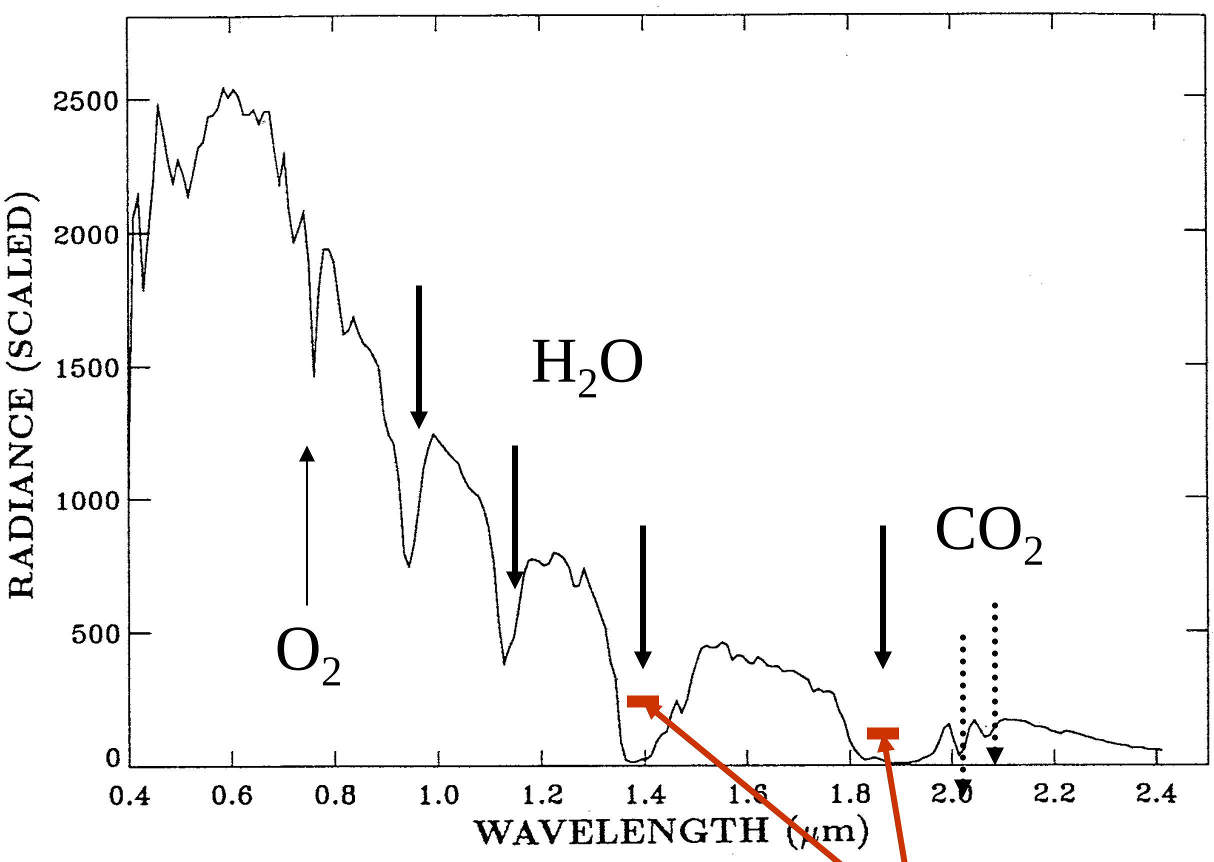

The AVIRIS spectrum is affected by atmospheric absorption and scattering effects. In order to obtain the surface reflectance spectrum, the atmospheric effects need to be removed.

Strong water vapor bands are located near 1.38 and 1.88 micron. No signals are detected under clear sky conditions.

Aerosol Scattering Effects
(Illustrated with AVIRIS RIM Fire Data)

True Color Image
(R: 0.64, G: 0.55, B: 0.46 μm)

False Color Image
(R: 2.13, G:1.24, B:1.64 μm)

B/W Single Channel Image
(0.37 μm)

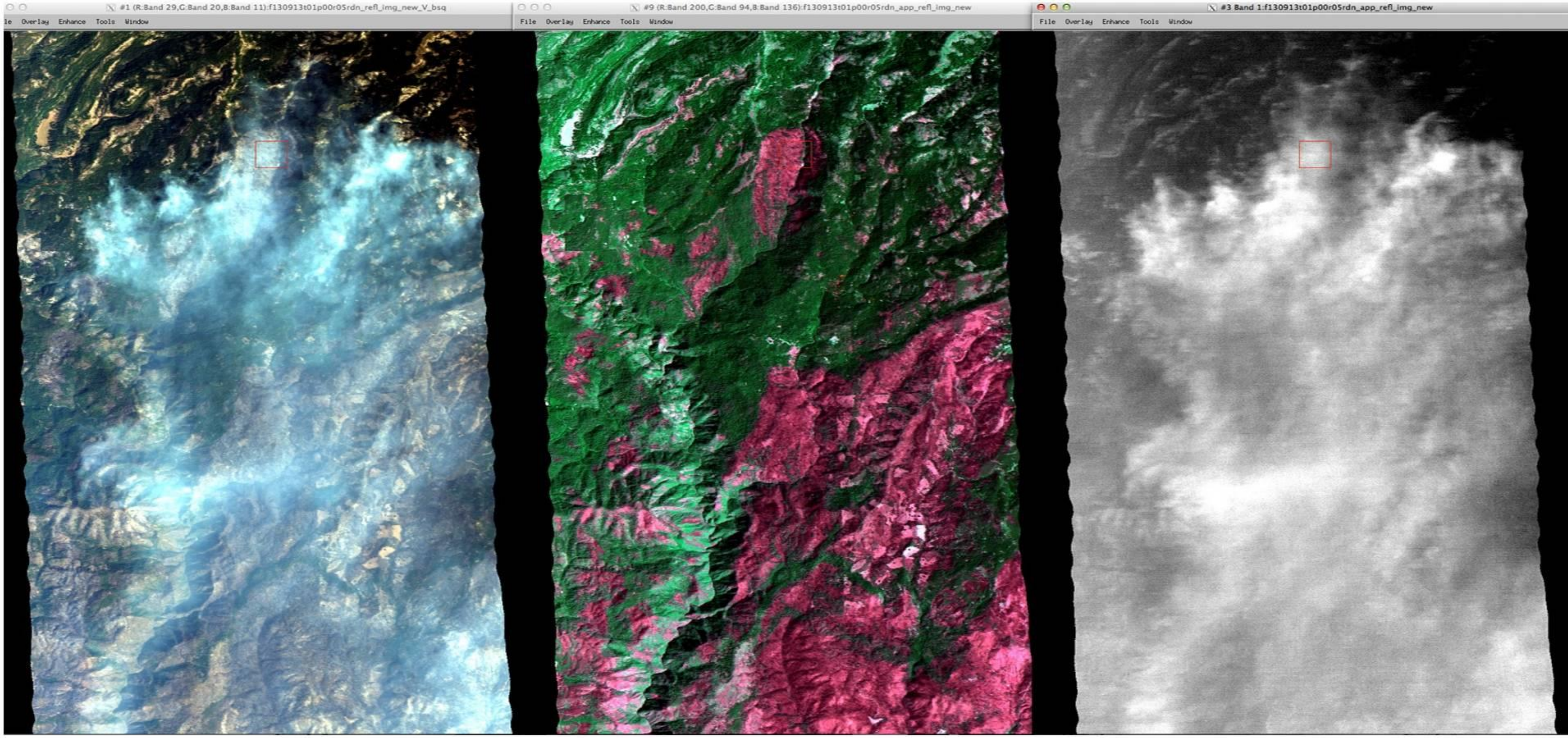

Smoke is seen in visible channel images, but disappears in the SWIR channel images. Smoke particle size is typically 0.1 – 0.2 μm. The UV channel at 0.37 μm is especially sensitive for smoke detection.

Equations and Definitions

The measured radiance at the satellite level can be expressed as:

$$L_{obs} = L_a + L_{sun}\ t\ \rho \qquad (1)$$

L_a: path radiance;
ρ : surface reflectance;
L_{sun}: solar radiance above the atmosphere;
t: *2-way transmittance for the Sun-surface-sensor path*

Define the satellite apparent reflectance as

$$\rho^*_{obs} = \pi\ L_{obs}\ /\ (\mu_0\ E_0) \qquad (2)$$

$$\rho^*_{obs} = T_g\ [\ \rho_a + t\ \rho\ /\ (1 - \rho\ s)\ ] \qquad (3)$$

By inverting Eq. (3) for ρ, we get:

$$\rho = (\rho^*_{obs}/T_g - \rho^*_a)\ /\ [t + s\ (\rho^*_{obs}/T_g - \rho^*_a)\ ] \qquad (4)$$

At present, we mainly use a modified version of 6S code to simulate atmospheric scattering effects (6S is fast). We also have a separate version of retrieving code using pre-computed lookup tables generated with a vector radiative transfer code.

(A caution on 5S & 6S users: V(km) → τ(550 nm) conversion in the subroutine "ODA550" is valid in the 5 – 23 km visibility range).

The Relative Importance of Aerosol Scattering and Absorption in Remote Sensing

ROBERT S. FRASER AND YORAM J. KAUFMAN

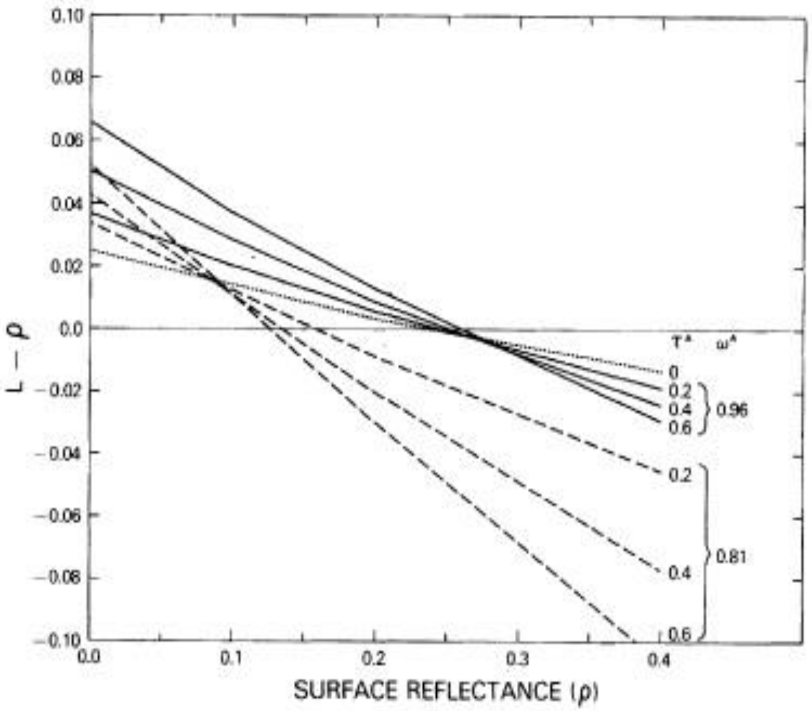

Fig. 2. The radiance of the Earth-atmosphere system minus the surface radiance (in reflectance units) for nadir observation, as a function of the surface reflectance. The total aerosol optical thickness τ^A and the single scattering albedo ω^A are indicated for each line. The solar zenith angle is 40°, the wavelength is 610 nm, and $\nu = 3$.

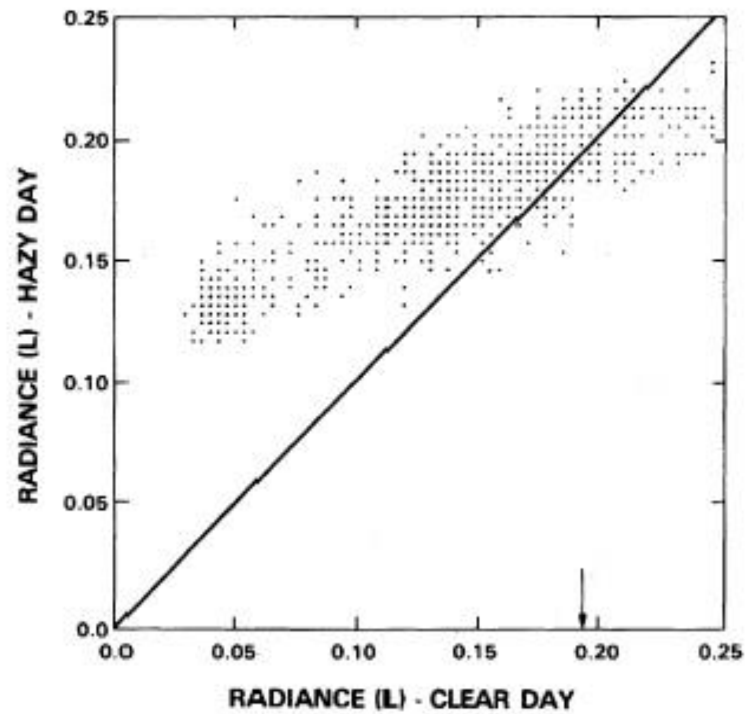

Fig. 5. Scatter diagram of the radiance from a Landsat image on a hazy day as a function of the radiance on a clear day taken over Washington, DC. The arrow indicates the radiance for which no change occurs due to the haziness difference between the clear and the hazy day. The waveband is 700–900 nm; solar zenith angle is 33°.

Atmospheric Gas Absorption

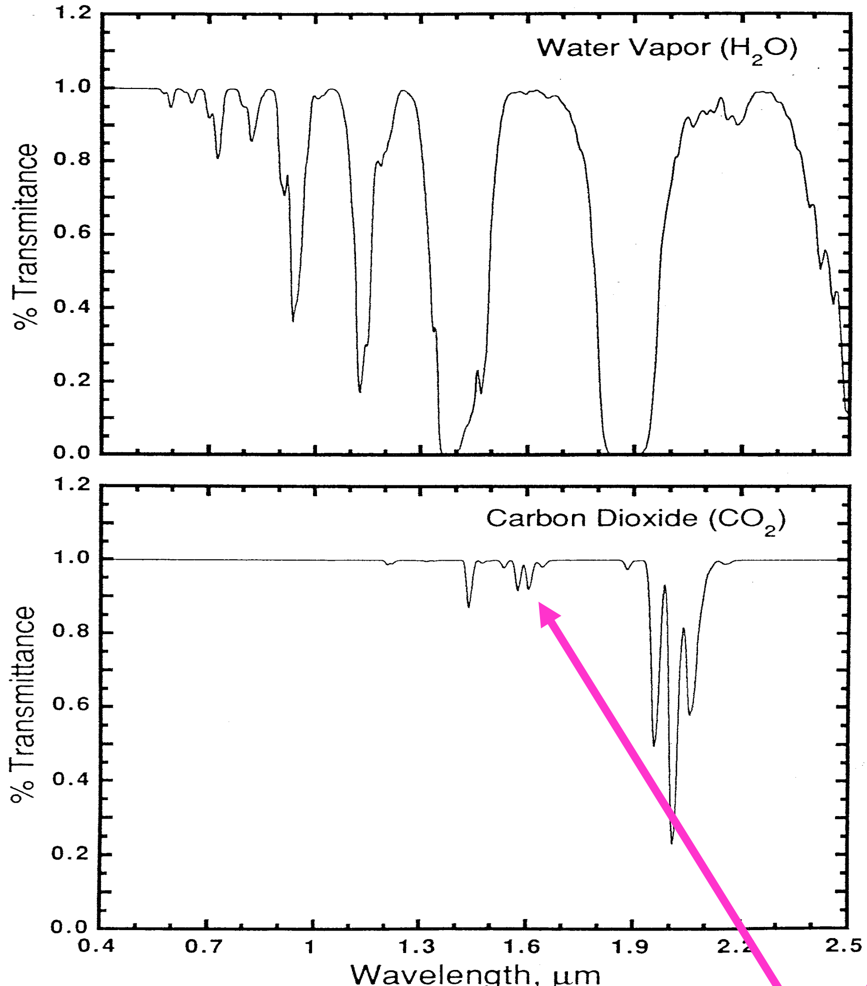

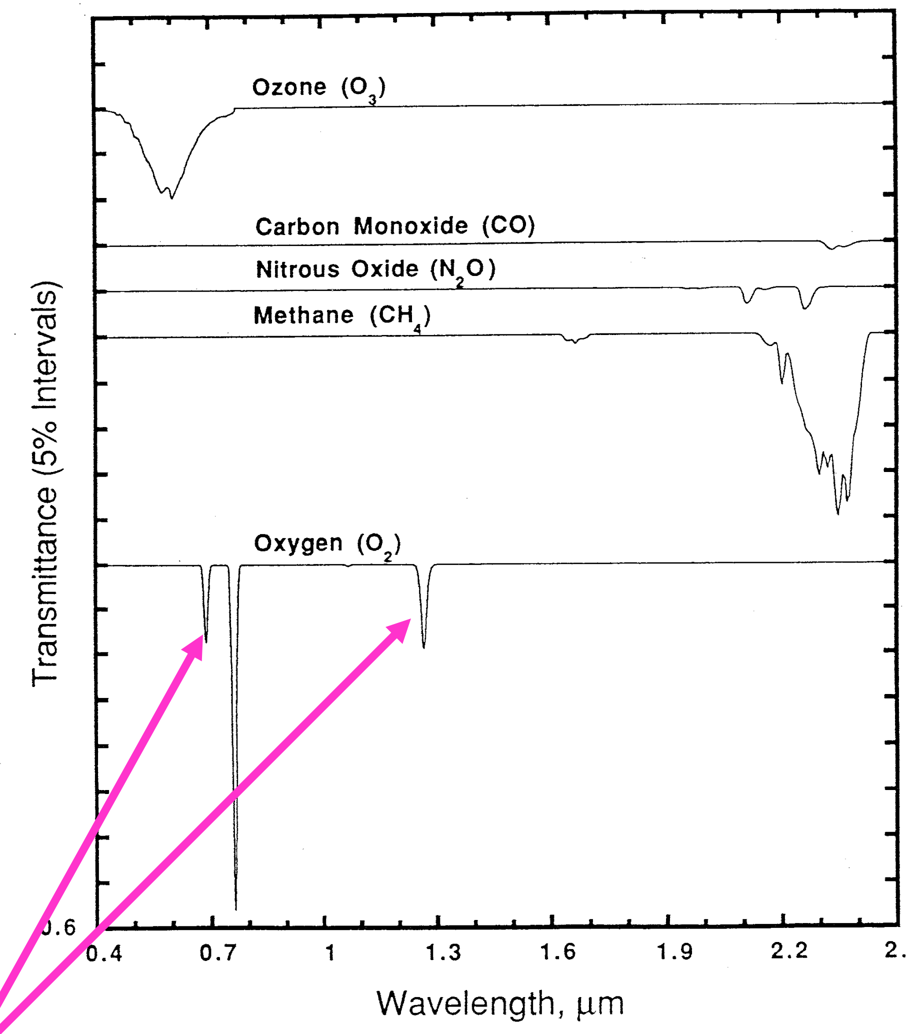

We have just realized that accurate modeling of these weak CO2 and O2 bands requires incorporation of new spectroscopy, such as line mixing, collision-induced absorption, non-Voigt line shape, etc.

Water Vapor & Vegetation Liquid Water Derivation Using Spectrum-Matching or Channel Ratio Techniques

Spectrum-Matching (a soil pixel)

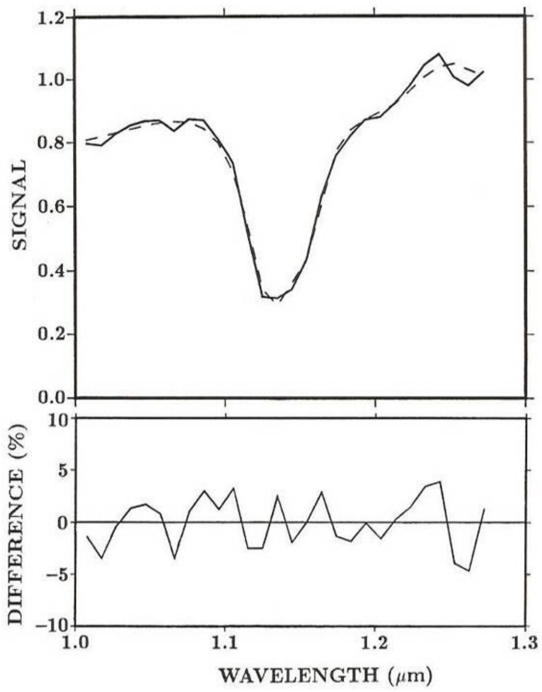

Spectrum-Matching (green vegetation)

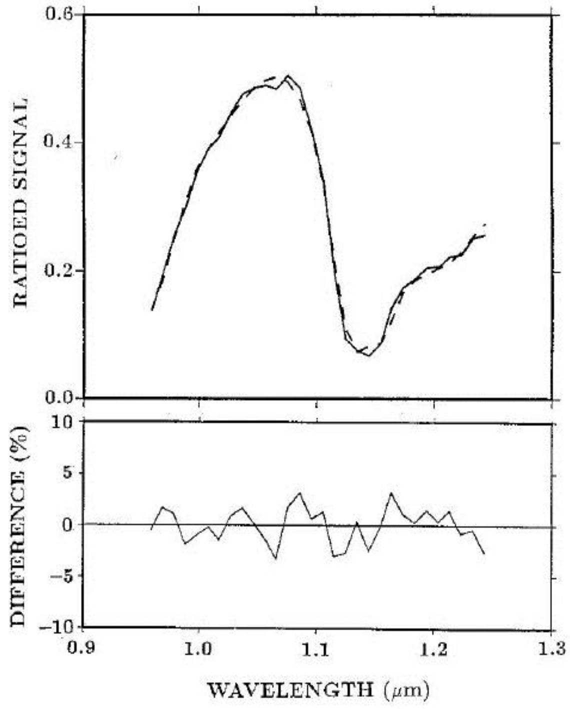

Channel Ratio

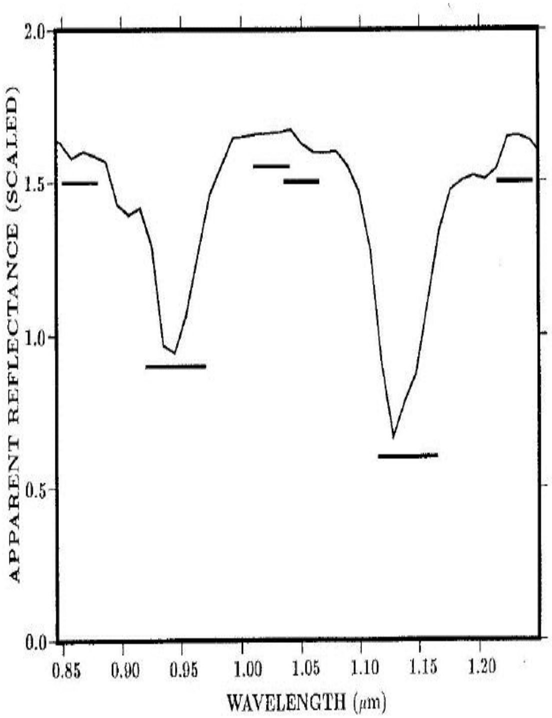

The sensitivity of the 0.94- and 1.14-micron water vapor bands and the surface reflectance properties allow us to retrieve water vapor amount using either spectrum-matching or channel ratio techniques. The water vapor effects in the entire 0.4 – 2.5 micron range can then be modeled and removed properly.

AVIRIS Image & Spectra Over Ivanpah, California (April 26, 2010)

FALSE COLOR IMAGE

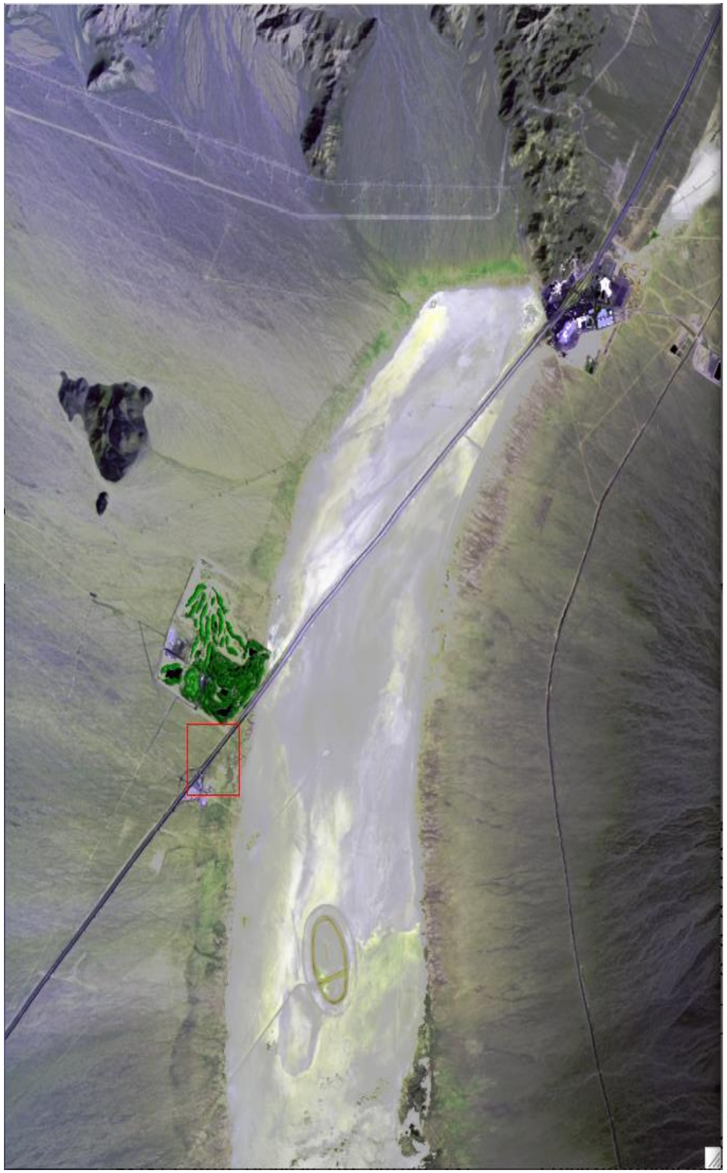

SAMPLE SPECTRA (Retrieved)

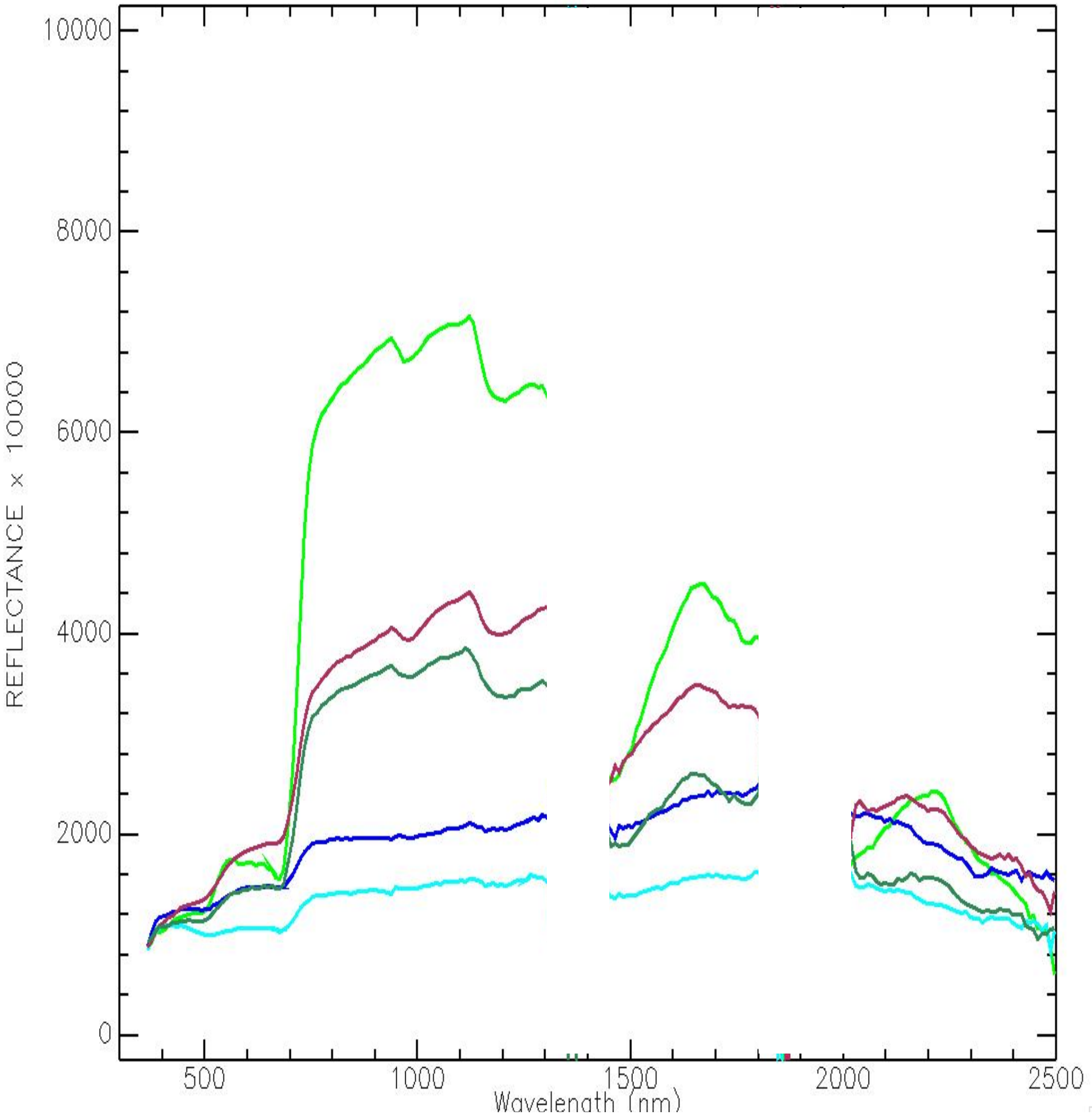

MINERAL MAPPING USING ATREM OUTPUT

by Scientists at USGS in Denver, Colorado

RGB Image (Cuprite, NV)

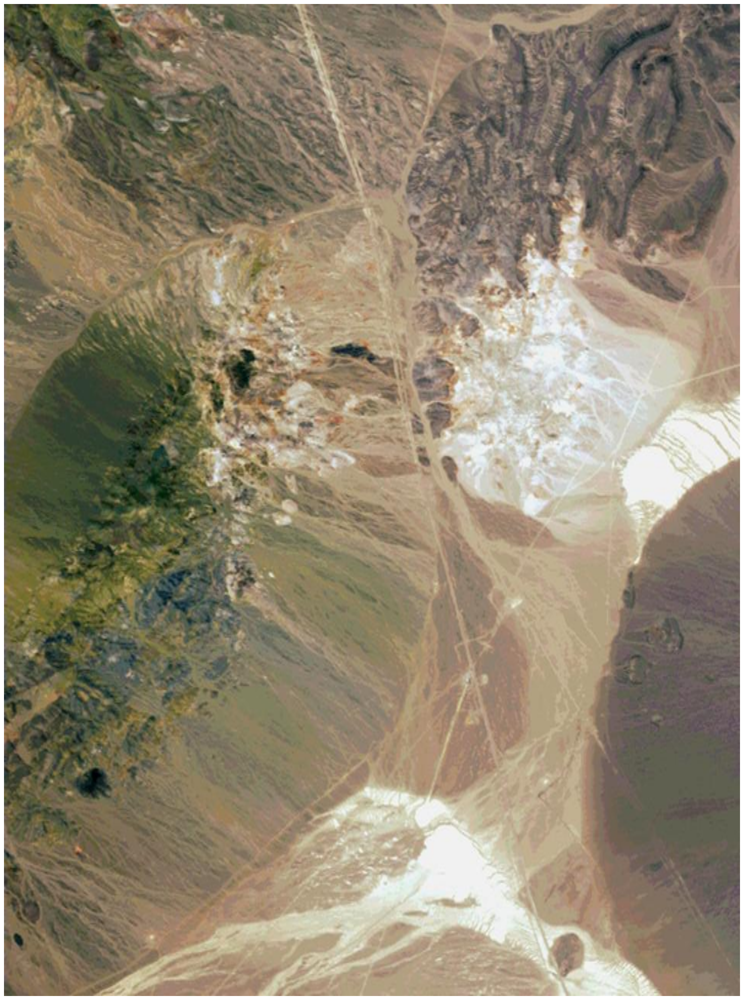

USGS Mineral Map, ~11x18 km

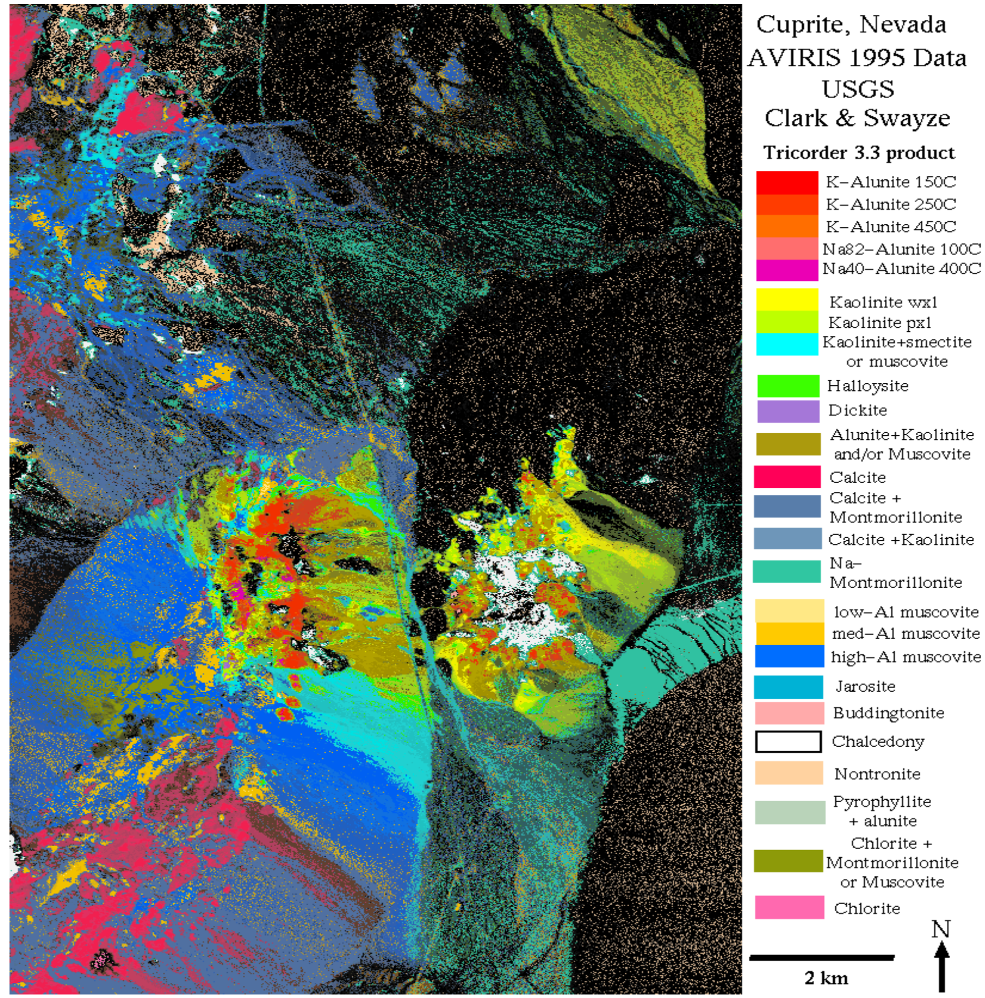

Cirrus Corrections

AVIRIS data acquired over Bowie, MD in summer 1997

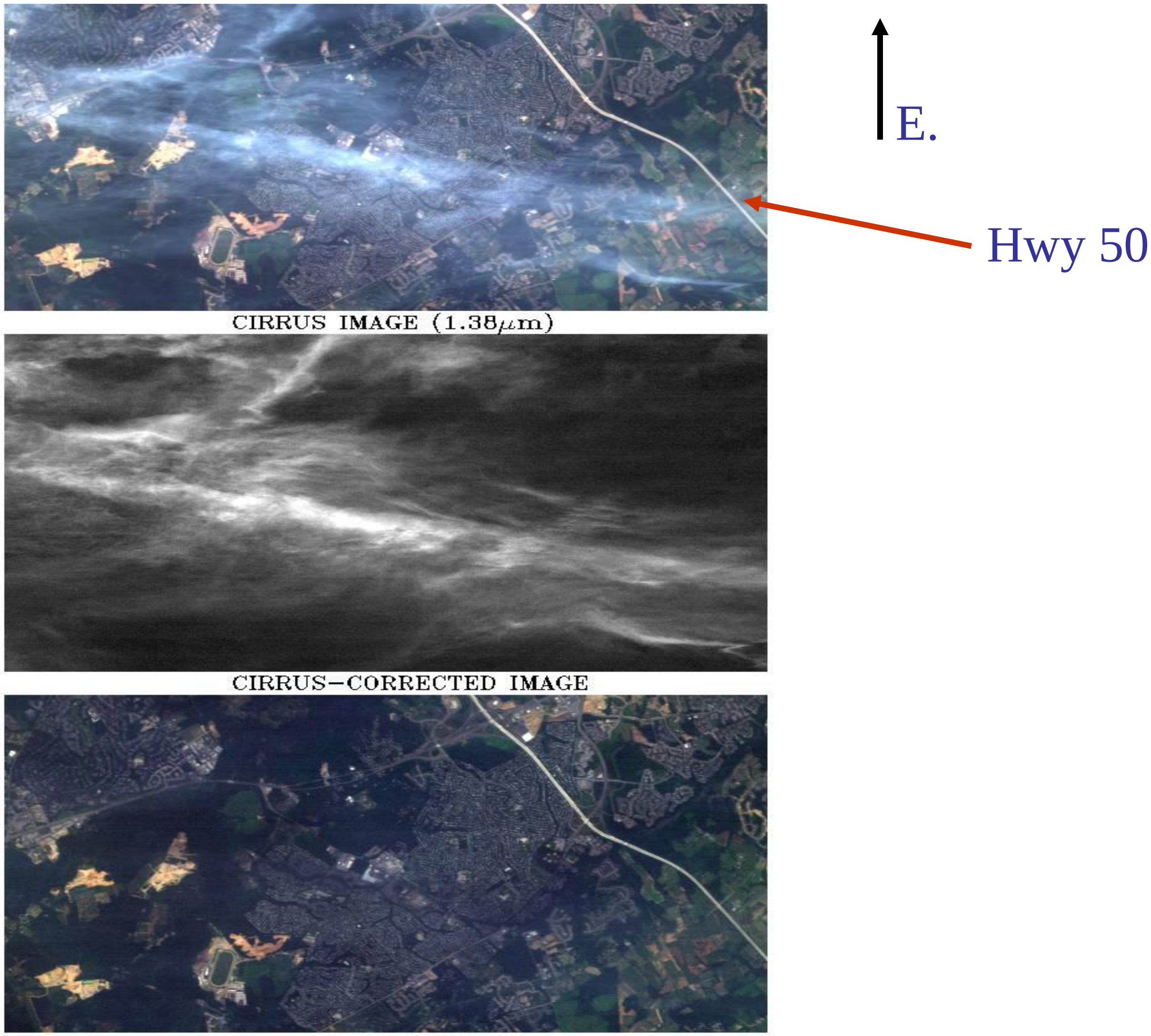

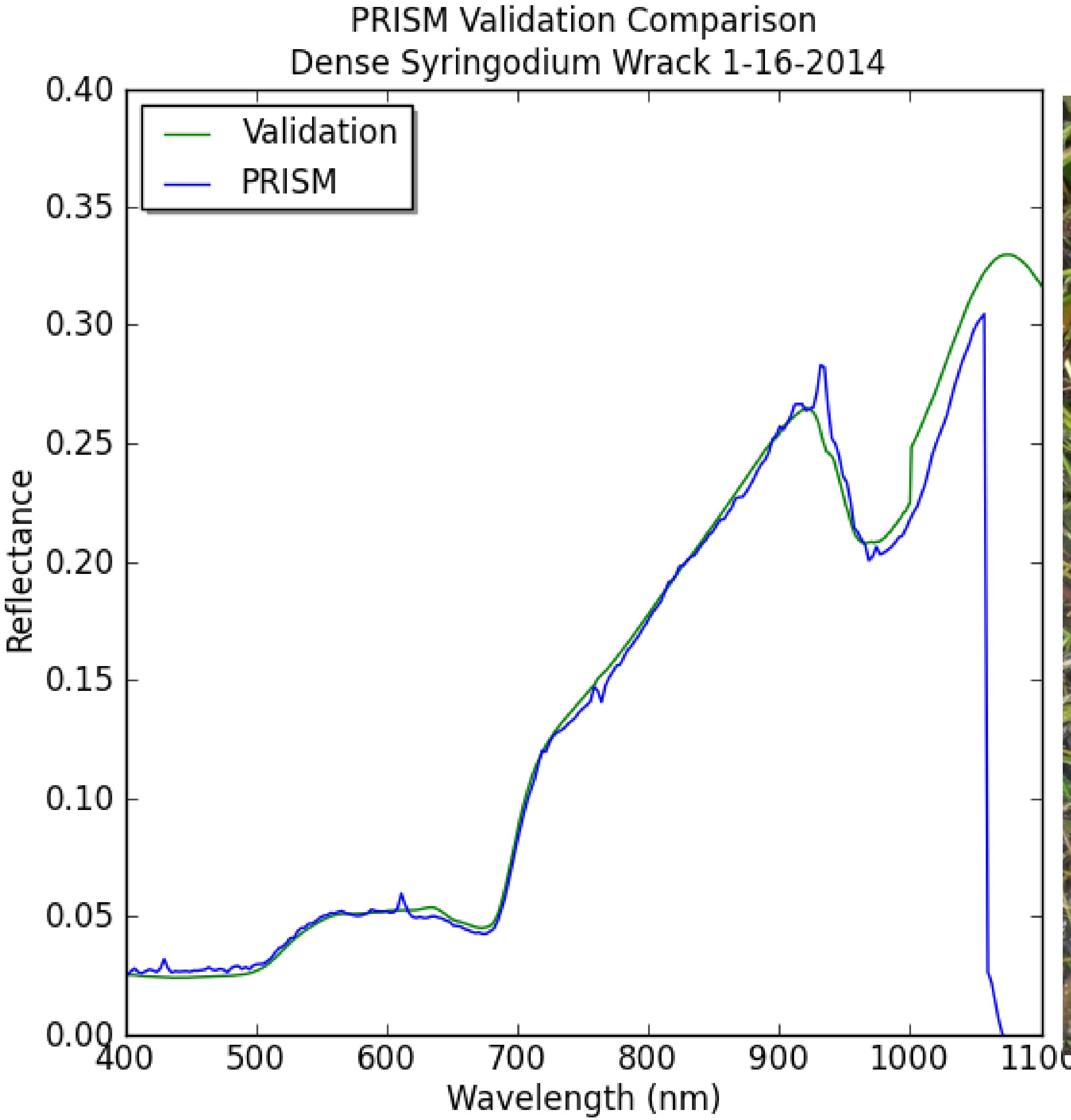
PRISM Validation Comparison
Dense Syringodium Wrack 1-16-2014
Validation
PRISM
Reflectance
Wavelength (nm)
0.00
0.05
0.10
0.15
0.20
0.25
0.30
0.35
0.40
400
500
600
700
800
900
1000
1100

A Sample Surface Reflectance Retrieval From JPL PRISM Data Having A Spectral Resolution of 3 nm

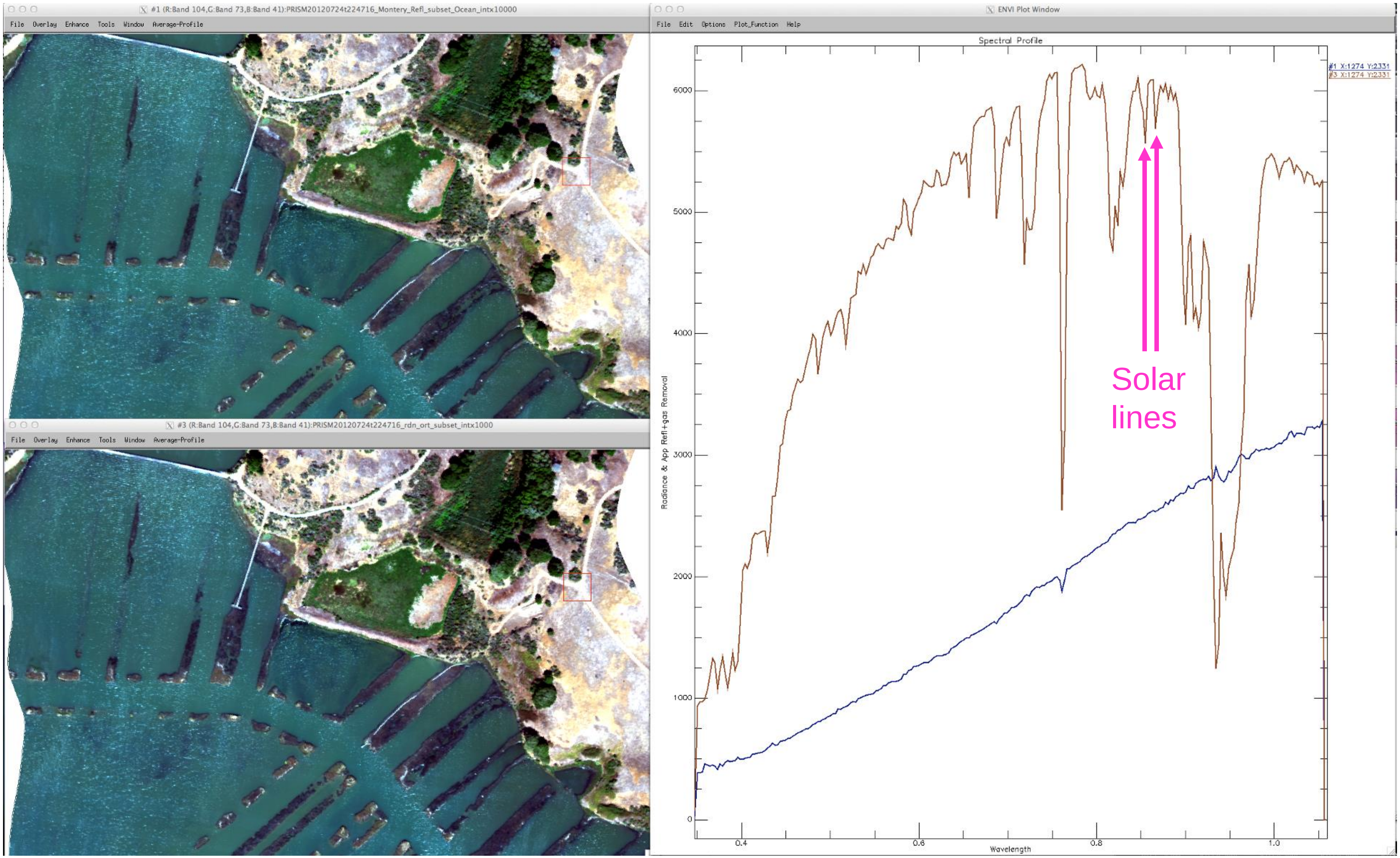

Discrepancy Among Standard Extra-Terrestrial Solar Irradiance Curves (Smoothed to the PRISM 3 nm Spectral Resolution)

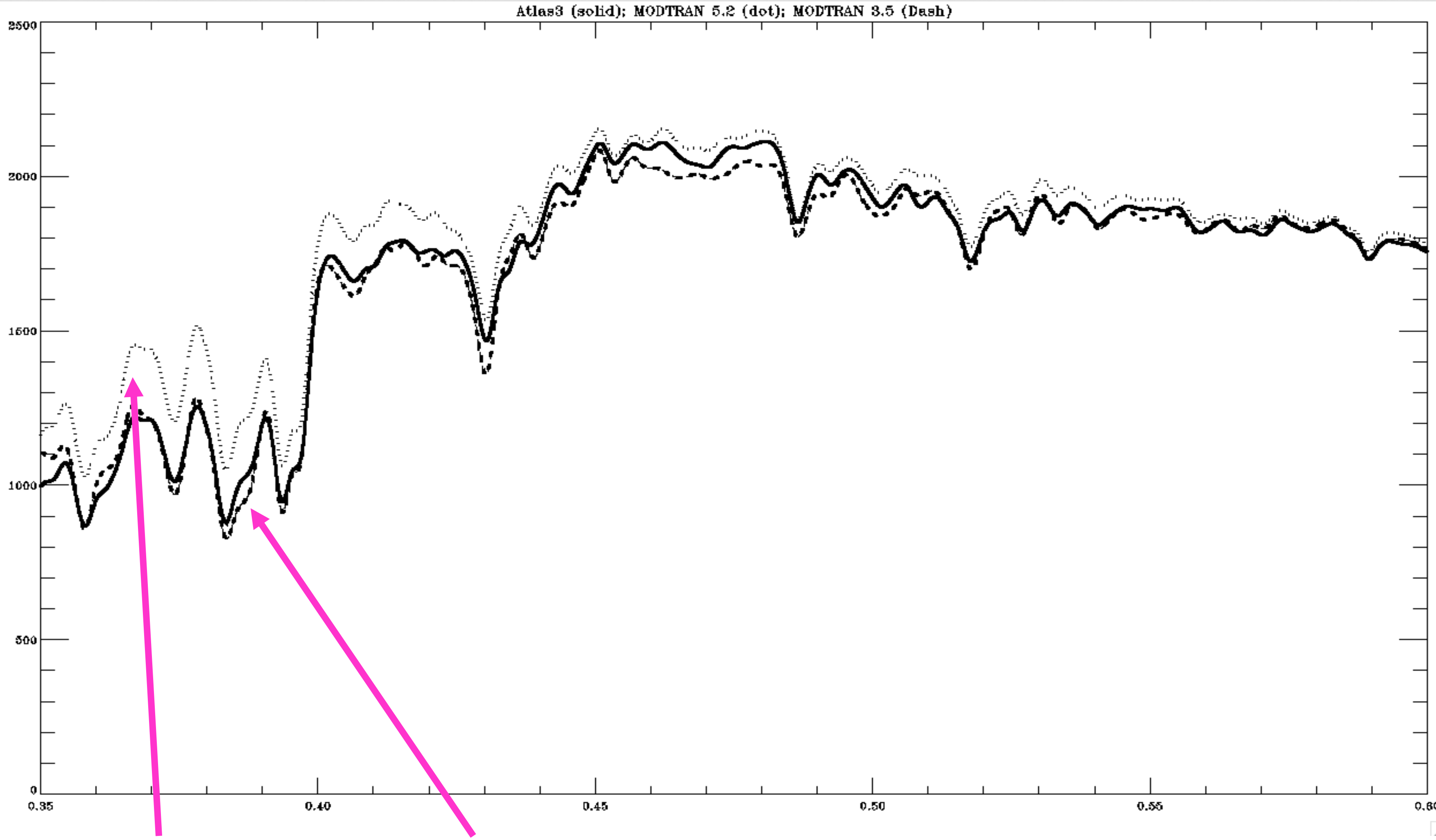

The magnitude and shapes of solar features in different solar curves do not agree. We need to have a very accurate solar irradiance curve to model PRISM types of data at a spectral resolution of 3 nm.

SUMMARY

- We have developed and improved hyperspectral atmospheric correction algorithms for remote sensing of land surfaces starting from the HIRIS era till present. A review paper on the subject was published in a 2009 special RSE issue in honoring of Professor Alex. Geotz.
- The same land algorithms plus an empirical sunglint correction module are also applicable for remote sensing of coastal waters from high spatial resolution hyperspectral imaging data.
- Our algorithms have been used for processing hyperspectral imaging data collected by a number of imaging spectrometers, including AVIRIS, TRWIS-III, CASI, HIDICE, EO-1/Hyperion, ISS/HICO, and most recently PRISM.
- In view of the recent development in atmospheric gas spectroscopy in the ultra spectral research community, we still need to improve techniques for modeling weak O_2 and CO_2 bands in NIR and SWIR spectral regions to include the effects of line mixing, non-Voigt line shape, and collision-induced-absorption.
- We also need an improved standard extra-terrestrial solar irradiance curve for better modeling of the PRISM data at a spectral resolution of 3 nm.

BACKUP SLIDES

Solar Irradiance Ratio Curves Published on *The Earth Observer*

The Earth Observer March - April 2014 Volume 26, Issue 2

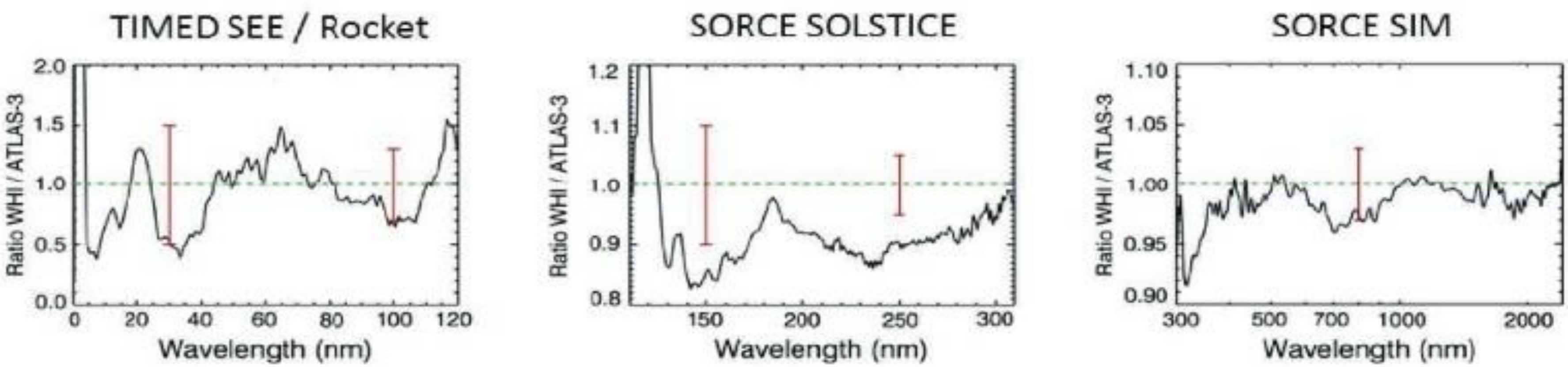

Figure 2. Comparison of irradiance levels from the Whole Heliospheric Interval (WHI) reference spectrum in April 2008 (measured during SC 23 minimum) relative to the ATLAS 3 reference spectrum of November 1994 (measured during SC 22 minimum). These three graphs cover the spectral range from X-rays to near-infrared wavelengths. The ratio of these two spectra—separated by 13 years—suggests lower irradiance values during the SC 23 minimum, but estimated errors of the two spectra make this lower value marginal at the 2σ uncertainty level. Notice the change in scale going from the highly variable extreme ultraviolet part of the spectrum (0-120 nm) to the very quiet visible and infrared spectral regimes (300-2000 nm). **Image credit:** Tom Woods [LASP/CU]

Remote Sensing of Environment 113 (2009) S17–S24

Contents lists available at ScienceDirect

Remote Sensing of Environment

journal homepage: www.elsevier.com/locate/rse

Atmospheric correction algorithms for hyperspectral remote sensing data of land and ocean

Bo-Cai Gao [a,*], Marcos J. Montes [a], Curtiss O. Davis [b], Alexander F.H. Goetz [c]

[a] Remote Sensing Division, Naval Research Laboratory, Washington, DC 20375 USA
[b] College of Oceanic and Atmospheric Sciences, Oregon State University, Corvallis, OR 97331 USA
[c] Analytical Spectral Devices, Inc., 5335 Sterling Drive, Boulder, CO 80301 USA

A R T I C L E I N F O

Article history:
Received 5 January 2007
Received in revised form 7 November 2007
Accepted 9 December 2007

Keywords:
Hyperspectral
Imaging spectrometer
Atmospheric correction
Remote sensing

A B S T R A C T

Hyperspectral imaging data have been collected with different types of imaging spectrometers from aircraft and satellite platforms since the mid-1980s. Because the solar radiation on the sun-surface-sensor path in the 0.4–2.5 μm visible and near-IR spectral regions is subject to absorption and scattering by atmospheric gases and aerosols, the hyperspectral imaging data contains atmospheric effects. In order to use hyperspectral imaging data for quantitative remote sensing of land surfaces and ocean color, the atmospheric effects must be removed. Over the years, atmospheric correction algorithms have evolved from the earlier empirical line method and the flat field method to more recent methods based on rigorous radiative transfer modeling approaches. Here, a review of hyperspectral atmospheric correction techniques is presented. Issues related to spectral smoothing are discussed. Suggestions for improvements to the present atmospheric correction